MYCOBIOLOGY
2022, VOL. 50, NO. 6, 420–428
https://doi.org/10.1080/12298093.2022.2152951

RESEARCH ARTICLE

OPEN ACCESS Check for updates

Five Previously Unrecorded Fungal Species Isolated from Marine Plastic Wastes in South Korea

Ji Seon Kim, Sung Hyun Kim, Wonjun Lee, Chang Wan Seo, Jun Won Lee, Ki Hyeong Park and Young Woon Lim

School of Biological Sciences and Institute of Microbiology, Seoul National University, Seoul, Korea

ABSTRACT

Plastic wastes have a negative impact on marine environments; however, they can be used as carbon sources and habitats by certain microbes. Microbes in the marine plastisphere can migrate worldwide through the ocean and cause serious environmental problems when they encounter suitable environments. Therefore, efforts to investigate the microbes inhabiting the marine plastisphere are increasing. In the present study, fungal strains were isolated from plastic wastes buried in Korean sea sands and mudflats and identified using molecular and morphological analyses. Five species were identified that were previously unrecorded from South Korea: *Cladosporium funiculosum*, *Neosetophoma poaceicola*, *Neosetophoma rosigena*, *Parasarocladium gamsii*, and *Trichoderma fomiticola*. Their molecular phylogenies and morphological characteristics are described in this study.

ARTICLE HISTORY
Received 29 August 2022
Revised 10 November 2022
Accepted 24 November 2022

KEYWORDS
Marine fungi; newly recorded species; phylogenetic analysis; plastisphere

1. Introduction

Plastics, being light, hard, and easily modifiable, are widely used in various fields, such as households, industry, agriculture, and fisheries. However, plastic wastes are difficult to decompose biologically, since plastics are resistant to degradation. Thus, plastic wastes have continued to accumulate in the environment. In 2020, 30 million tons of post-consumer plastic wastes were collected from Europe alone [1]. Traditional disposal methods, such as recycling and littering, have become ineffective because of the large amount of accumulated plastic wastes. Up to one million tons of improperly dumped plastic wastes that originate on land are carried into the ocean by the wind or rivers [2]. This has become so severe that an island of plastic wastes has formed in the ocean, which affects all marine organisms both physically and chemically [3]. However, certain microbes can use this plastic waste island as their habitat [4,5]. Researchers have acknowledged plastic environments as a type of ecosystem called "plastisphere" [6].

Numerous studies on microorganisms in plastispheres from various environments, including freshwater [7,8] and land [9,10] have been conducted. However, the marine plastisphere has received comparatively less attention [11,12], despite being the first plastisphere to be discovered [13]. Marine plastic wastes differ significantly from terrestrial plastic wastes. Microbes in the marine plastisphere can migrate worldwide through marine plastic garbage drifts, and some can act as opportunistic pathogens when they encounter a suitable environment [14,15]. Therefore, efforts to identify the microbes inhabiting the marine plastisphere are increasing [16]. Many bacteria associated with the plastic wastes in the marine environment have been discovered [17,18]. However, relatively little research has been conducted on fungi living on marine plastic wastes, although approximately 1,800 marine fungi have been reported to date (https://marinefungi.org, accessed on August 22, 2022). Recently, fungi associated with plastic debris have been reported using metabarcoding [19,20]. Fungi may play an important ecological role in the plastisphere, since some fungi can break down plastics [21–23]. A culturomics approach is required to isolate fungi inhabiting marine plastic wastes and to evaluate their plastic-degrading ability.

Recently, we investigated the fungal diversity in a marine plastisphere based on culturomics and evaluated their ability to degrade polycaprolactone (PCL) [24] as part of the Marine Fungal Resource Bank project. While conducting this diversity study, we identified five species that were recorded for the first time in South Korea. Their detailed morphological and molecular characteristics are described in the present study.

CONTACT Young Woon Lim ywlim@snu.ac.kr

2. Materials and methods

2.1. Sampling and fungal isolation

Polyethylene terephthalate (PET) plastic wastes buried in mudflats and sea sand were collected from six sites in South Korea in April 2018 (Table 1, Figure 1). After sampling, decontamination and fungal isolation process were performed as described in the previous research [24]. Pure fungal isolates were stored in 20% (v/v) glycerol at −80 °C and deposited in the Seoul National University Fungus Collection (SFC).

2.2. Molecular analyses

For molecular analyses, the genomic DNA of each fungal strain was extracted using the modified cetyltrimethylammonium bromide extraction protocol [25]. All strains were initially identified using internal transcribed spacer (ITS) region sequences. To obtain ITS sequences, PCR was conducted using the primer set ITS1F [26]/ITS4 [27] in a C1000 thermal cycler (Bio-Rad, Richmond, CA, USA). The PCR conditions were as follows: initial denaturation at 95 °C for 5 min; 35 cycles of denaturation at 95 °C for 40 s, annealing at 55 °C for 40 s, and extension at 72 °C for 60 s; and a final extension at 72 °C for 5 min. The PCR products were purified using the Expin™ PCR Purification Kit (GeneAll Biotechnology, Seoul, South Korea), according to the manufacturer's guidelines. Sequencing was performed using an ABI 3730xL DNA Analyzer (Life Technologies, Gaithersburg, MD, USA) at Macrogen (Seoul, South Korea).

All sequences were proofread using FinchTV v.1.4 and identified using BLAST in NCBI (https://blast.ncbi.nlm.nih.gov/Blast.cgi). Species identification was assigned to species with over 97% similarity in BLAST using the NCBI database. For accurate identification of the species, the RAxML phylogenetic analysis of the ITS region for each genus was conducted using reference sequences from GenBank. The actin (*act*) and RNA polymerase II subunit B (*rpb2*) regions of *Cladosporium* and *Trichoderma*, respectively, were additionally amplified in the same way as described above for accurate species identification. ACT-512F/ACT-783R [28] or ACT1Fd/ACT1Rd [29] for *act* and fRPB2-5F/fRPB2-7cR [30] for *rpb2* were used as the primer sets. The subsequent process was the same as described above. All sequences produced in this study were deposited in GenBank (Table 2). All multiple alignments were performed using MAFFT v.7 [31] with default options. By using RAxML [32], maximum likelihood analyses were performed in the CIPRES web portal [33] with the general time-reversible model GTR + GAMMA with 1,000 bootstrap replicates.

2.3. Morphological observation

Morphological observations of the five newly recorded species were performed according to previous studies [34–39]. The description procedure for *Neosetophoma* and *Parasarocladium* has not yet been standardized [34,37,39]. Therefore, potato dextrose agar (PDA), oatmeal agar (OA), and malt extract agar (MEA), purchased from BD Difco™

Table 1. Species identification results and sampling site information of the fungal strains discovered in this study.

Species	Strain No.	Sampling location	Latitude	Longitude
Cladosporium funiculosum	SFC20220715_M07	Jangmok-ri, Jangmok-myeon, Geoje-si, Gyeongsangnam-do	34°59′36.1"	128°40′30.7"
Neosetophoma poaceicola	SFC20220715_M06	Wonpyeong-ri, Yongnam-myeon, Tongyeong-si, Gyeongsangnam-do	34°45′46.2"	127°34′44.4"
Neosetophoma rosigena	SFC20220715_M03	Jinseo-ri, Jinseo-myeon, Buan-gun, Jeollabuk-do	35°35′38.5"	126°36′12.8"
Parasarocladium gamsii	SFC20220715_M04	Gwanpo-ri, Jangmok-myeon, Geoje-si, Gyeongsangnam-do	34°59′7.9"	128°41′49.7"
	SFC20220715_M10	Dongdal-ri, Yongnam-myeon, Tongyeong-si, Gyeongsangnam-do	34°51′57.13"	128°27′7.24"
Trichoderma fomiticola	SFC20220715_M01	Masan-ri, Byeollyang-myeon, Suncheon-si, Jeollanam-do	34°50′25.53"	127°26′52.04"

Figure 1. Photos illustrating an example of the PET plastic wastes sampled in this study.

Table 2. The strains and their GenBank accession numbers used for phylogenetic analyses in this study.

Species	Strain No.	ITS	*act*	*rpb2*
Brunneomurispora lonicerae	KUMCC 18-0157	NR_164299	–	–
Cercospora beticola	CBS 116456	–	AY840458	–
Cladosporium australiense	CBS 125984	–	HM148486	–
Cladosporium cavernicola	URM 8389	–	MZ555746	–
Cladosporium crousii	CBS 140686	–	LN834615	–
Cladosporium endoviticola	JZB390018	–	MN984220	–
Cladosporium funiculosum	CBS 122129	NR_119845	HM148583	–
	SFC20220715_M07	**OP070802**	**OP022380**	–
Cladosporium gamsianum	CBS 125989	–	HM148584	–
Cladosporium macadamiae	BRIP 72269a	–	MZ344214	–
Cladosporium needhamense	CBS 143359	–	MF473991	–
Cladosporium phaenocomae	CBS 128769	–	JF499881	–
Cladosporium pseudocladosporioides	CBS 125993	–	HM148647	–
Cladosporium uredinicola	CPC 5390	–	HM148712	–
Cladosporium uwebraunianum	CBS 143365	–	OU641392	–
Cladosporium verrucocladosporioides	CBS 126363	–	HM148717	–
Cladosporium welwitschiicola	CPC 18648	–	KY646226	–
Hypocrea estonica	CBS 121556	–	–	FJ860536
Hypocrea fomiticola	C.P.K. 3137	–	–	FJ860539
Hypocrea moravica	C.P.K. 954	–	–	FJ860547
	C.P.K. 2419	–	–	FJ860548
	C.P.K. 2489	–	–	FJ860549
Hypocrea phyllostachydis	CBS 114071	–	–	FJ860570
Hypocrea strictipilosa	C.P.K. 1601	–	–	FJ860594
Neosetophoma guiyangensis	GZCC 18-0111	MH018134	–	–
Neosetophoma lonicerae	KUMCC 18-0155	NR_164444	–	–
Neosetophoma miscanthi	FU31023	MK503820	–	–
Neosetophoma phragmitis	CBS 145364	MK539954	–	–
Neosetophoma poaceicola	MFLUCC 16-0886	NR_165861	–	–
	SFC20220715_M06	**OP070784**	–	–
Neosetophoma rosae	MFLUCC 15-0682	KU302779	–	–
Neosetophoma rosigena	MFLU 17-0626	NR_157525	–	–
	SFC20220715_M03	**OP070764**	–	–
Neosetophoma samarorum	CBS 138.96	MH862569	–	–
Neosetophoma xingrensis	GZCC 18-0110	MH018135	–	–
Parasarocladium aestuarinum	CMG30	MK986714	–	–
	CMG31	MK986714	–	–
Parasarocladium alavariense	CMG32	MK986715	–	–
	CMG34	MK986718	–	–
Parasarocladium fusiforme	CMG37	MK986720	–	–
	CMG38	MK986725	–	–
	CMG39	MK986724	–	–
Parasarocladium gamsii	CBS 726.71	NR_159615	–	–
	SFC20220715_M04	**OP070778**	–	–
	SFC20220715_M10	**OP223413**	–	–
	CR1_9	MK460909	–	–
Parasarocladium radiatum	CBS 142.62	MH424699	–	–
Parasarocladium tasmanniae	CPC 38162	MW175340	–	–
Parasarocladium wereldwijsianum	NL19094001	MW883438	–	–
Sarocladium strictum	CBS 346.70	MH871457	–	–
Trichoderma ceramicum	CBS 114576	–	–	FJ860531
Trichoderma fertile	DAOM 167070	–	–	AF545545
	DAOM 167161	–	–	AF545546
Trichoderma fomiticola	CBS 121136	NR_134391	–	FJ860538
	SFC20220715_M01	**OP070730**	–	**OP255996**
Trichoderma hunanense	HMAS:248841	–	–	KY687980
Trichoderma longipile	GJS 91-93	–	–	AF545512
Trichoderma oblongisporum	DAOM 167085	–	–	AF545551
Trichoderma parestonicum	CBS 120636	–	–	FJ860565
Trichoderma spirale	CBS 136472	–	–	KJ665348
Trichoderma thailandicum	GJS 97-61	–	–	AY391957

(Sparks, MD, USA), were used as defaults for the morphological observation of all species belonging to those genera. Cultivations of *Cladosporium* were conducted on synthetic nutrition-poor agar (SNA; KH_2PO_4 1 g, KNO_3 1 g, KCl 0.5 g, Glucose 0.2 g, Saccharose 0.2 g, Bacto agar (Difco, Detroit, MI, USA) 20 g per 1 L) [38] as well as the default media. *Trichoderma* was cultivated on PDA, corn meal agar (CMD; Difco, Detroit, MI, USA), and SNA [40]. All cultures were incubated at 25 °C for 7 days, and the hyphal growth of *Trichoderma* was measured daily starting from the third day post-incubation to evaluate the fungal growth rate. The Methuen Handbook of Color was used to determine the name and alphanumerical number of each colony color [41]. The microscopic observation for *Trichoderma* was processed under a light microscope (Eclipse 80i, Nikon, Tokyo, Japan) with strains growth on PDA and CMD for 7 days, and for *Cladosporium*, strains growth on SNA for 7 days at 25 °C on the dark were used [38]. ImageJ was used to measure the colony diameter [42].

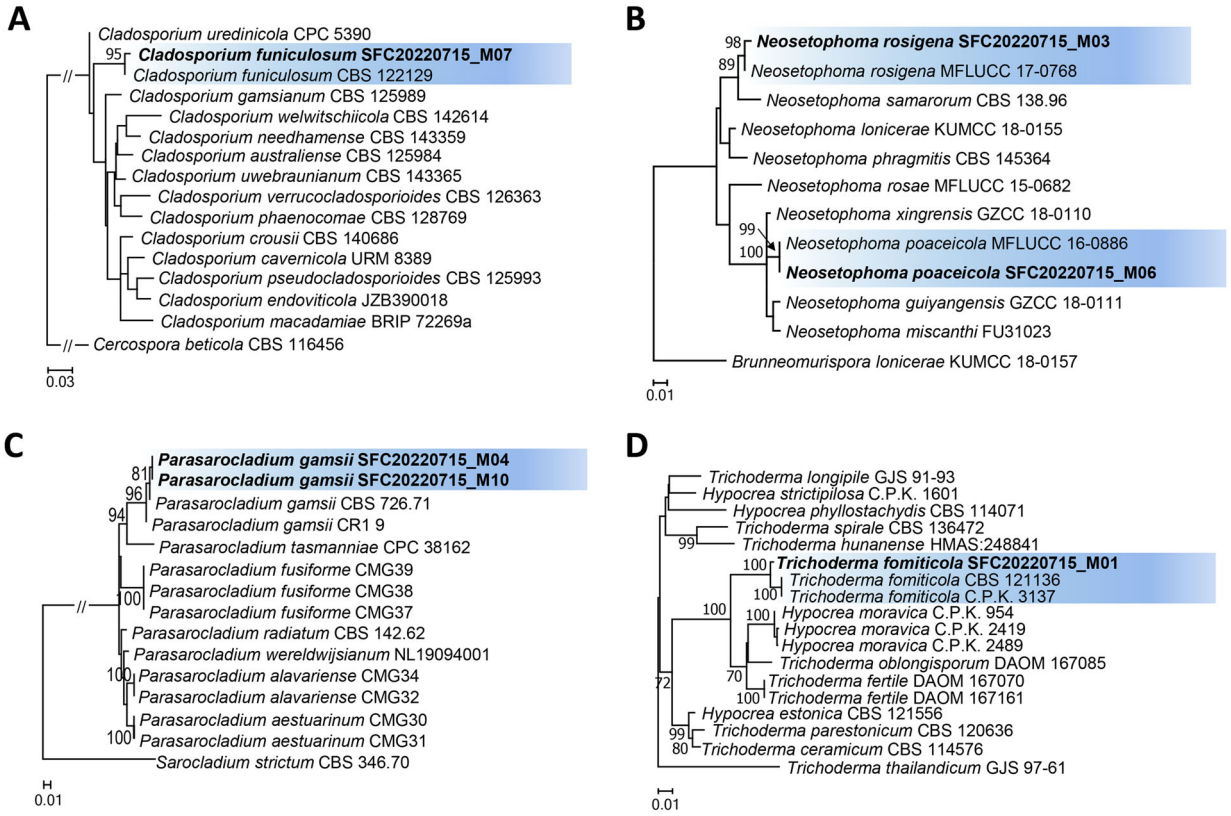

Figure 2. Maximum likelihood phylogenetic trees of (A) *Cladosporium* based on *act*, (B) *Neosetophoma* based on ITS, (C) *Parasarocladium* based on ITS, and (D) *Trichoderma* clade *Semiorbis* based on *rpb2*. Bootstrap values over 70 are presented at the nodes. The scale bar represents the number of nucleotide substitutions per site. The species discovered in this study are included in the blue boxes, and the sequences newly conducted in this study were highlighted in bold.

3. Results

3.1. Species identification

Six fungal strains were isolated from the marine PET plastic wastes (Figure 1, Table 1). Through molecular identifications based on the ITS sequences of these strains, four strains were identified into three species: *Neosetophoma poaceicola* (SFC20220715_M06) (Figure 2(B)), *Neosetophoma rosigena* (SFC20220715_M03) (Figure 2(B)), and *Parasarocladium gamsii* (SFC20220715_M04 and SFC20220715_M10) (Figure 2(C)). The remaining two strains, SFC20220715_M01 and SFC20220715_M07, were morphologically identified at the genus level as *Trichoderma* and *Cladosporium*, respectively. To identify the species, protein-coding genes were used. Finally, SFC20220715_M07 was identified as *Cladosporium funiculosum* based on its conidia shape, dark green colony, and ITS and *act* region sequences (Figure 2(A)). SFC20220715_M01 was identified as *Trichoderma fomiticola* based on its conidia shape, grayish yellow colony, and ITS and *rpb2* region sequences (Figure 2(D)).

Phylogenetic analysis revealed that SFC20220715_M07, classified in *Cladosporium*, formed a monophyletic group with *C. funiculosum* CBS 122129 (sequence similarity for *act* = 99.4%; bootstrap support = 100%). SFC20220715_M06 and SFC20220715_M03, classified in *Neosetophoma*, clustered with the type strains of *N. poaceicola* (MFLUCC 16-0886) (sequence similarity for ITS = 99%; bootstrap support = 99%) and *N. rosigena* (MFLUCC 17-0768) (sequence similarity for ITS = 99.6%; bootstrap support = 99%), respectively. SFC20220715_M04 formed a clade with the type strain (CBS 726.71) of *P. gamsii* (sequence similarity for ITS = 99.6%; bootstrap support = 96%). Finally, SFC20220715_M01 formed a distinct monophyletic group with two strains (CBS 121136 and C.P.K. 3137) of *T. fomiticola* (sequence similarity for *rpb2* = 99%).

3.2. Taxonomy

***Cladosporium funiculosum* W. Yamam** (1959) (Figures 2(A) and 3(A))

Description: Colony diam, 7 d, in mm: PDA 25 °C 33–35; MEA 25 °C 26–34; OA 25 °C 26–37.

Colony characteristics: PDA, 25 °C, 7 d: Colonies low, flat; margins low, radially sulcate, entire; mycelia white; texture velvety; sporulation dense; conidia dark green (29F4); exudates absent;

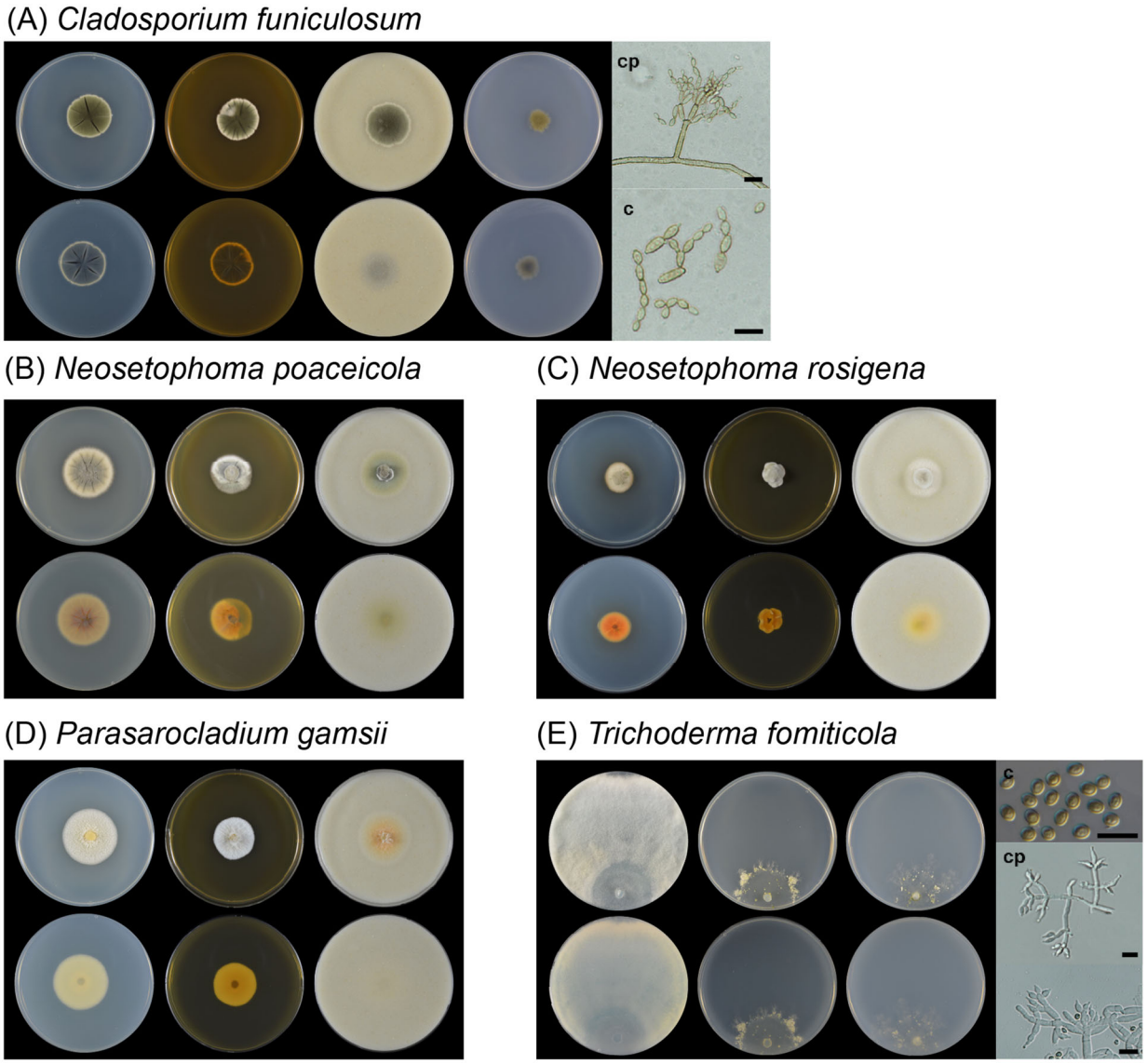

Figure 3. Morphological characteristics of the five fungal species recorded in this study. (A) Colonies after 7 days at 25 °C, from left to right potato dextrose agar (PDA), malt extract agar (MEA), oatmeal agar (OA), and synthetic nutrition-poor agar (SNA); (B–D) Colonies after 7 days at 25 °C, from left to right PDA, MEA, and OA; (E) Colonies after 7 days at 25 °C, from left to right PDA, corn meal dextrose agar (CMD), and SNA. Abbreviations: cp conidiophore, c for conidia.

soluble pigments absent; reverse color grayish turquoise (24E4). MEA, 25 °C, 7 d: Colonies low, radially sulcate; margins low, wide, entire; mycelia white; texture velvety; sporulation dense; conidia dark green (29F4); exudates absent; soluble pigments absent; reverse color dark brown (6F8). OA, 25 °C, 7 d: Colonies low, flat; margins low, wide, entire; mycelia white; texture velvety; sporulation dense; conidia dull green (29D4); exudates absent; soluble pigments absent; reverse color dull green (29D4). SNA, 25 °C, 7 d: Colonies low, flat; margins low, narrow, entire; mycelia white; texture velvety; sporulation moderate; conidia grayish yellow (3C4); exudates absent; soluble pigments absent; reverse color olive (3F3).

Mycelium composed of septate, branched, hyaline to subhyaline, sometimes olivaceous, verruculose to verrucose hyphae, 2–4.5 μm wide. Conidiophores macronematous, sometimes reduced to conidiogenous cells, septate, erect or somewhat slightly flexuous, usually unbranched, up to 180 μm long, 3–4 μm wide, pale brown, verruculose to verrucose. Conidiogenous cells integrated, terminal or intercalary, cylindrical, 18–48 × 2.5–4.5 μm, bearing up to 3 conidiogenous loci, slightly darkened and refractive. Ramoconidia 0–1(–4)-septate, cylindrical, 15–36 × 2.7–4.3 μm [av. (± SD) 26 (± 5.95) × 3.3 (± 0.37)], pale brown, verruculose to verrucose. Conidia forming branched chains, with up to eight conidia in the terminal unbranched part, sometimes long neck between conidia, 0(–1) septate, pale brown, verruculose to verrucose, slightly darkened and refractive. Small terminal conidia aseptate, ellipsoidal, 2.6–4.8 × 1.4–2.4 μm [av. (± SD) 4.8 (± 0.57) × 1.8

(± 0.28)]. Intercalary conidia 0(–1) septate, ellipsoidal to subcylindrical, 3.5–12.1 × 1.7–3.4 μm [av. (± SD) 6.6 (± 2.4) × 2.4 (± 0.37)]. Secondary ramoconidia 0(–1) septate, subcylindrical to cylindrical, 7.7–25.6 μm long × 2.1–3.6 μm [av. (± SD) 13.7 (± 4.51) × 2.8 (± 0.35)].

Strain examined: SFC20220715_M07, isolated from plastic wastes in mudflats in South Korea.

Note: SFC20220715_M07 is morphologically similar to the type strain CBS 122129 of *Cladosporium funiculosum*, except for the following features [38]. SFC20220715_M07 had darker conidia on PDA and did not have aerial mycelium on MEA, whereas the type strain had more light-colored conidia, such as grayish olive conidia on PDA [38].

***Neosetophoma poaceicola* Goonas., Thambug. & K.D. Hyde (2017)** (Figures 2(B) and 3(B))

Description: Colony diam, 7 d, in mm: PDA 25 °C 32–33; MEA 25 °C 25–27; OA 25 °C 31–33.

Colony characteristics: PDA, 25 °C, 7 d: Colonies low, radially sulcate; margins low, wide, entire; mycelia yellowish white (4A2); texture floccose; sporulation moderate; conidia brownish grey (4D2); exudates absent; soluble pigments absent; reverse color orange (5A5) at the center, pale orange (5A3) elsewhere. MEA, 25 °C, 7 d: Colonies low, radially sulcate; margins low, wide, entire; mycelia white; texture floccose; sporulation moderate; conidia grey (5C1); exudates absent; soluble pigments absent; reverse color orange (5A7). OA, 25 °C, 7 d: Colonies low, flat; margins low, wide, entire; mycelia white; texture velvety to floccose; sporulation moderate; conidia grayish green (29B4); exudates absent; soluble pigments absent; reverse color pale green (29A3).

Strain examined: SFC20220715_M06, isolated from plastic wastes in sea sands in South Korea.

Note: Current morphological descriptions of *N. poaceicola* focus mainly on sexual morphs, leaving the asexual morphs relatively understudied. The growth rates of SFC20220715_M06 on PDA and OA were similar to those of the strain IRAN 2429 C, which is not a type strain [39]. Furthermore, the colony color of SFC20220715_M06 on PDA was similar (grayish) to that of IRAN 2439 C but different on OA, with SFC20220715_M06 exhibiting grayish green conidia and IRAN 2429 C was colorless.

***Neosetophoma rosigena* Wanas., E.B.G. Jones & K.D. Hyde (2018)** (Figures 2(B) and 3(C)).

Description: Colony diam, 7 d, in mm: PDA 25 °C 16–21; MEA 25 °C 15–17; OA 25 °C 23–26.

Colony characteristics: PDA, 25 °C, 7 d: Colonies low, flat; margins low, wide, entire; mycelia orange white (5A2); texture velvety; sporulation weak; exudates absent; soluble pigments grayish brown (5D3); reverse color deep orange (5A8). MEA, 25 °C, 7 d: Colonies low, flat; margins low, wide, entire; mycelia white; texture velvety; no sporulation; exudates absent; soluble pigments absent; reverse color deep orange (5A8). OA, 25 °C, 7 d: Colonies low, flat; margins low, wide, entire; mycelia white; texture velvety at the center, floccose elsewhere; no sporulation; exudates absent; soluble pigments absent; reverse color light yellow (4A5).

Strain examined: SFC20220715_M03, isolated from plastic wastes in mudflats in South Korea.

Note: The overall characteristics of the strain SFC20220715_M03 resembled those of the type strain MFLUCC 17-0768: they shared the same color and texture of conidia. However, SFC20220715_M03 exhibited a relatively faster growth rate and sporulation than the type strain [37].

***Parasarocladium gamsii* (Tichelaar) Summerb., J.A. Scott, Guarro & Crous (2018)** (Figures 2(C) and 3(D))

Description: Colony diam, 7 d, in mm: PDA 25 °C 33–35; MEA 25 °C 26–34; OA 25 °C 26–37.

Colony characteristics: PDA, 25 °C, 7 d: Colonies low, flat; margins low, wide, entire; mycelia white; texture velvety to floccose; no sporulation; exudates absent; soluble pigments absent; reverse color pale yellow (4A3). MEA, 25 °C, 7 d: Colonies low, flat; margins low, wide, entire; mycelia white; texture floccose; no sporulation; exudates absent; soluble pigments absent; reverse color orange (5A6). OA, 25 °C, 7 d: Colonies low, flat; margins low, wide, entire; mycelia white; texture floccose; sporulation moderate; conidia light orange (5A4); exudates absent; soluble pigments absent; reverse color cannot be observed.

Strains examined: SFC20220715_M04, isolated from plastic wastes in mudflat in South Korea. SFC20220715_M10, isolated from plastic wastes in sea sands in South Korea.

Note: The overall morphological characteristics of SFC20220715_M04 and SFC20220715_M10 were similar to those of the type strain CBS 726.71. However, there was a difference in the margin characteristics: the type strain CBS 726.71 was irregular [34] and SFC20220715_M04 was entire.

***Trichoderma fomiticola* Jaklitsch** (2009) (Figures 2(D) and 3(E))

Description: Optimum growth at 25 °C on all media, 7 d, in mm: CMD 25 °C 23–26; PDA 25 °C 47–52; OA 25 °C 22–33.

Colony characteristics: CMD, 25 °C, 7 d: Aerial mycelium sparse; cottony pustules forming on the margin of the colony, conidia forming sparsely, grayish yellow (2B4); no distinctive odor; no soluble pigments. PDA, 25 °C, 7 d: Aerial mycelium

abundant; cottony, conidia forming sparsely, with broad concentric rings, white; no distinctive odor; no soluble pigments. SNA, 25 °C, 7 d: Aerial mycelium sparse; cottony pustules forming around the inoculum, conidia forming sparsely, grayish green (30D5); no distinctive odor; no soluble pigments.

Stipe width 2.9–4.1 μm. Branches forming regular trees, narrow, paired. Phialides 2.3–4.0 × 5.1–10.2 μm, variable, lageniform, thicker in or below the middle, ampulliform. Conidia 3.6–4.9 × 2.9–4.1 μm, yellowish green to dark green, smooth, subglobose to ellipsoidal.

Strain examined: SFC20220715_M01, isolated from plastic wastes in mudflat in South Korea.

Note: The type strain CBS 121136 of *Trichoderma fomiticola* produced strong sporulation on PDA. However, SFC20220715_M01 exhibited relatively weak sporulation. Additionally, the growth rate of SFC20220715_M01 on all media was considerably slower than that of the type strain [40].

4. Discussion

Five previously unrecorded species were discovered from marine plastispheres buried in mudflats and sea sand in South Korea. They were identified primarily through maximum likelihood phylogenetic analysis of the ITS sequences. Other protein-coding genes were additionally used for identifying *C. funiculosum* and *T. fomiticola* because of the low resolution of their ITS sequences. The *act* and *rpb2* genes were proposed as specific markers for *Cladosporium* [38] and *Trichoderma* [30], respectively. Subsequently, using morphological analysis based on colony characteristics, these species were confirmed to be previously unrecorded from South Korea and belonged to three orders: Cladosporiales, Pleosporales, and Hypocreales.

The morphological features of the five species differed depending on both culture methods and ecological characteristics. We observed that the growth morphologies of *C. funiculosum* and *T. fomiticola* were identical to those of their corresponding type strains because *Cladosporium* and *Trichoderma* have well-established culture methods [38,40]. *Neosetophoma poaceicola* and *N. rosigena* isolated from plastic wastes showed differences in morphological characteristics, such as growth rates and colony colors, when compared with the reference strains [37,43]. The reference species were reported from their plant hosts: *N. poaceicola* from dead grass [43] and apple leaf [39] and *N. rosigena* from *Rosa* [37]. Their cultural methods have not yet been standardized. The present study is the first to report these species from plastisphere, which is an artificial environment. Fungal morphology can vary depending on the nutritional components, water capacity, and artificial media types [44–46]. Morphological differences may result from different habitats and the lack of standardized cultural methods.

The plastic-degrading ability of the five species was evaluated using PCL agar (Kim et al. [24]). The species could degrade plastic but were categorized as weak PCL degraders. These species are known as saprobes or pathogens. For example, *C. funiculosum* [38] and *N. poaceicola* [43,47] are saprobes as well as a plant pathogen [39], and *N. rosigena* is a saprobe [37]. Hydrolases and oxidoreductases of saprobic and pathogenic fungi are crucial for the degradation of lignocellulose [48] or pathogenesis [49]. Fungi containing various enzymes can biodegrade plastic substances [50]. Therefore, the five species isolated from the plastisphere may possess enzymes that can degrade plastics.

In conclusion, we discovered five plastic-associated fungi from marine environments, which were not previously reported from South Korea. These species can use plastics as their habitat and carbon source. Their cultural morphologies vary depending on their habitat—whether they are living in a natural or man-made environment. Standard culture methods for the species *P. gamsii*, *N. poaceicola*, and *N. rosigena* are unknown, making the comparison of morphological differences between strains isolated from different environments challenging. Thus, our report on their growth features will help to establish standard cultural methods in the future. Furthermore, these species have the potential to be used in various fields because of their plastic-degrading abilities in marine environments.

Disclosure statement

No potential conflict of interest was reported by the author(s).

Funding

This study was supported by the National Marine Biodiversity Institute of Korea [2022M01100].

ORCID

Ji Seon Kim http://orcid.org/0000-0003-1869-7347
Sung Hyun Kim http://orcid.org/0000-0002-5505-9451
Wonjun Lee http://orcid.org/0000-0002-7227-0777
Chang Wan Seo http://orcid.org/0000-0002-5948-1836
Jun Won Lee http://orcid.org/0000-0003-1416-3428
Ki Hyeong Park http://orcid.org/0000-0002-8832-7643
Young Woon Lim http://orcid.org/0000-0003-2864-3449

References

[1] Plastics Europe. Plastics-the Facts 2021. 2021.
[2] Lebreton L, Van Der Zwet J, Damsteeg JW, et al. River plastic emissions to the world's oceans. Nat Commun. 2017;8(1):1–10.
[3] Kühn S, Van Franeker JA. Quantitative overview of marine debris ingested by marine megafauna. Mar Pollut Bull. 2020;151:110858.
[4] Amaral-Zettler LA, Zettler ER, Mincer TJ. Ecology of the plastisphere. Nat Rev Microbiol. 2020;18(3): 139–151.
[5] Li C, Wang L, Ji S, et al. The ecology of the plastisphere: microbial composition, function, assembly, and network in the freshwater and seawater ecosystems. Water Res. 2021;202:117428.
[6] Zettler ER, Mincer TJ, Amaral-Zettler LA. Life in the "plastisphere": microbial communities on plastic marine debris. ES. Environ Sci Technol. 2013; 47(13):7137–7146.
[7] Barros J, Seena S. Plastisphere in freshwaters: an emerging concern. Environ Pollut. 2021;290: 118123.
[8] González-Pleiter M, Velázquez D, Casero MC, et al. Microbial colonizers of microplastics in an arctic freshwater lake. Sci Total Environ. 2021;795: 148640.
[9] Rüthi J, Bölsterli D, Pardi-Comensoli L, et al. The "plastisphere" of biodegradable plastics is characterized by specific microbial taxa of alpine and arctic soils. Front Environ Sci. 2020;8:562263.
[10] MacLean J, Mayanna S, Benning LG, et al. The terrestrial plastisphere: diversity and polymer-colonizing potential of plastic-associated microbial communities in soil. Microorganisms. 2021;9(9): 1876.
[11] Jacquin J, Cheng J, Odobel C, et al. Microbial ecotoxicology of marine plastic debris: a review on colonization and biodegradation by the "plastisphere. Front Microbiol. 2019;10:865.
[12] Du Y, Liu X, Dong X, et al. A review on marine plastisphere: biodiversity, formation, and role in degradation. Comput Struct Biotechnol J. 2022;20: 975–988.
[13] Carpenter EJ, Smith K. Jr. Plastics on the sargasso sea surface. Science. 1972;175(4027):1240–1241.
[14] Wright RJ, Erni-Cassola G, Zadjelovic V, et al. Marine plastic debris: a new surface for microbial colonization. Environ Sci Technol. 2020;54(19): 11657–11672.
[15] Zhu D, Ma J, Li G, et al. Soil plastispheres as hotspots of antibiotic resistance genes and potential pathogens. Isme J. 2022;16(2):521–532.
[16] Gkoutselis G, Rohrbach S, Harjes J, et al. Microplastics accumulate fungal pathogens in terrestrial ecosystems. Sci Rep. 2021;11(1):1–13.
[17] Kumari A, Chaudhary DR, Jha B. Destabilization of polyethylene and polyvinylchloride structure by marine bacterial strain. Environ Sci Pollut Res Int. 2019;26(2):1507–1516.
[18] Devi RS, Ramya R, Kannan K, et al. Investigation of biodegradation potentials of high density polyethylene degrading marine bacteria isolated from the coastal regions of Tamil Nadu, India. Mar Pollut Bull. 2019;138:549–560.
[19] De Tender C, Devriese LI, Haegeman A, et al. Temporal dynamics of bacterial and fungal colonization on plastic debris in the North sea. Environ Sci Technol. 2017;51(13):7350–7360.
[20] Davidov K, Iankelevich-Kounio E, Yakovenko I, et al. Identification of plastic-associated species in the mediterranean sea using DNA metabarcoding with nanopore MinION. Sci Rep. 2020;10(1):1–11.
[21] Yamada-Onodera K, Mukumoto H, Katsuyaya Y, et al. Degradation of polyethylene by a fungus, *Penicillium simplicissimum* YK. Polym Degrad Stab. 2001;72(2):323–327.
[22] Kanelli M, Vasilakos S, Nikolaivits E, et al. Surface modification of poly (ethylene terephthalate) (PET) fibers by a cutinase from *Fusarium oxysporum*. Process Biochem. 2015;50(11):1885–1892.
[23] Muhonja CN, Makonde H, Magoma G, et al. Biodegradability of polyethylene by bacteria and fungi from Dandora dumpsite Nairobi-Kenya. PLoS One. 2018;13(7):e0198446.
[24] Kim SH, Lee JW, Kim JS, et al. Plastic-inhabiting fungi in marine environments and PCL degradation activity. Antonie Van Leeuwenhoek. 2022; 115:1379–1392.
[25] Rogers SO, Bendich AJ. Extraction of total cellular DNA from plants, algae and fungi. Plant molecular biology manual. Dordrecht: Springer; 1994. p. 183–190.
[26] Gardes M, Bruns TD. ITS primers with enhanced specificity for basidiomycetes-application to the identification of mycorrhizae and rusts. Mol Ecol. 1993;2(2):113–118.
[27] White TJ, Bruns T, Lee S, et al. Amplification and direct sequencing of fungal ribosomal RNA genes for phylogenetics. PCR Protocols: A Guide to Methods and Applications. 1990;18(1):315–322.
[28] Carbone I, Kohn LM. A method for designing primer sets for speciation studies in filamentous ascomycetes. Mycologia. 1999;91(3):553–556.
[29] Groenewald J, Nakashima C, Nishikawa J, et al. Species concepts in *Cercospora*: spotting the weeds among the roses. Stud Mycol. 2013;75(1):115–170.
[30] Cai F, Druzhinina IS. In honor of john bissett: authoritative guidelines on molecular identification of *Trichoderma*. Fungal Divers. 2021;107(1):1–69.
[31] Katoh K, Standley DM. MAFFT multiple sequence alignment software version 7: improvements in performance and usability. Mol Biol Evol. 2013; 30(4):772–780.
[32] Stamatakis A. RAxML-VI-HPC: maximum likelihood-based phylogenetic analyses with thousands of taxa and mixed models. Bioinformatics. 2006; 22(21):2688–2690.
[33] Miller MA, Pfeiffer W, Schwartz T. The CIPRES science gateway: enabling high-impact science for phylogenetics researchers with limited resources. In Proceedings of the 1st Conference of the Extreme Science and Engineering Discovery Environment: bridging from the extreme to the campus and beyond, 2012. p. 1–8
[34] Tichelaar G. *Acremonium gamsii* nov. sp. (hyphomycetes). Acta Bot Neerl. 1972;21(3):197–199.
[35] Bustamante DE, Calderon MS, Leiva S, et al. Three new species of *Trichoderma* in the Harzianum and Longibrachiatum lineages from Peruvian cacao crop soils based on an integrative approach. Mycologia. 2021;113(5):1056–1072.

[36] Bensch K, Groenewald J, Meijer M, et al. *Cladosporium* species in indoor environments. Stud Mycol. 2018;89:177–301.
[37] Wanasinghe DN, Phukhamsakda C, Hyde KD, et al. Fungal diversity notes 709–839: taxonomic and phylogenetic contributions to fungal taxa with an emphasis on fungi on rosaceae. Fungal Divers. 2018;89(1):1–236.
[38] Bensch K, Braun U, Groenewald JZ, et al. The genus *Cladosporium*. Stud Mycol. 2012;72(1): 1–401.
[39] Ebrahimi L, Fotouhifar KB. First report of *Neosetophoma poaceicola* on apple leaf from Iran. J Crop Prot. 2021;10(2):450–457.
[40] Jaklitsch WM. European species of *Hypocrea* part I. The green-spored species. Stud Mycol. 2009;63:1–91.
[41] Kornerup A, Wanscher J. Methuen handbook of colour. 3rd ed. London: e. Methuen and Co Ltd. 1978.
[42] Schneider CA, Rasband WS, Eliceiri KW. NIH image to ImageJ: 25 years of image analysis. Nat Methods. 2012;9(7):671–675.
[43] Thambugala K, Wanasinghe D, Phillips A, et al. Mycosphere notes 1–50: grass (Poaceae) inhabiting Dothideomycetes. Mycosphere. 2017;8(4):697–796.
[44] Ahamed A, Vermette P. Effect of culture medium composition on *Trichoderma reesei*'s morphology and cellulase production. Bioresour Technol. 2009; 100(23):5979–5987.
[45] Sharma G, Pandey R. Influence of culture media on growth, colony character and sporulation of fungi isolated from decaying vegetable wastes. J Yeast Fungal Res. 2010;1(8):157–164.
[46] Sikder M, Mallik MRI, Alam N. Identification and in vitro growth characteristics of entomopathogenic fungus-*Aschersonia* sp. in Bangladesh. azb. 2019;7(1):11–18.
[47] Tennakoon DS, Thambugala KM, Wanasinghe DN, et al. Additions to Phaeosphaeriaceae (Pleosporales): *Elongaticollum* gen. nov., *Ophiosphaerella taiwanensis* sp. nov., *Phaeosphaeriopsis beaucarneae* sp. nov. and a new host record of *Neosetophoma poaceicola* from Musaceae. MycoKeys. 2020;70:59–88.
[48] Daly P, Cai F, Kubicek CP, et al. From lignocellulose to plastics: knowledge transfer on the degradation approaches by fungi. Biotechnol Adv. 2021; 50:107770.
[49] Arya GC, Cohen H. The multifaceted roles of fungal cutinases during infection. JoF. 2022;8(2):199.
[50] Temporiti MEE, Nicola L, Nielsen E, et al. Fungal enzymes involved in plastics biodegradation. Microorganisms. 2022;10(6):1180.